Numerical simulation of a green monopropellant for spacecraft application

Quentin Levard, Neven Louis, N. Pelletier, Duc Minh Le, Olivier Rouzaud, Christine Lempereur, Jouke Hijlkema, Jean-Yves Lestrade, Jerôme Anthoine

NUMERICAL SIMULATION OF A GREEN MONOPROPELLANT FOR SPACECRAFT APPLICATION

SPACE PROPULSION 2018
BARCELO RENACIMIENTO HOTEL, SEVILLE, SPAIN / 14 – 18 MAY 2018

Levard Q. (1), **Louis N.** (2), **Pelletier N.** (3), **Le D.M.** (4), **Rouzaud O.** (5), **Lempereur C.** (6), **Hijlkema J.** (7), **Lestrade J-Y** (8), **Anthoine J.** (9)

(1) *ONERA / DMPE, Université de Toulouse, F-31410 Mauzac, France - quentin.levard@onera.fr*
(2) *ONERA / DMPE, Université de Toulouse, F-31410 Mauzac, France - neven.louis@onera.fr*
(3) *CNES, 18 Avenue Edouard Belin, 31400 Toulouse, France - nicolas.pelletier@cnes.fr*
(4) *ONERA / DMPE, Université de Toulouse, F-31410 Mauzac, France - minh.le_duc@onera.fr*
(5) *ONERA / DMPE, Université de Toulouse, F-31055 Toulouse, France - olivier.rouzaud@onera.fr*
(6) *ONERA / DMPE, Université de Toulouse, F-31055 Toulouse, France - christine.lempereur@onera.fr*
(7) *ONERA / DMPE, Université de Toulouse, F-31410 Mauzac, France - jouke.hijlkema@onera.fr*
(8) *ONERA / DMPE, Université de Toulouse, F-31410 Mauzac, France - jean-yves.lestrade@onera.fr*
(9) *ONERA / DMPE, Université de Toulouse, F-31410 Mauzac, France - jerome.anthoine@onera.fr*

KEYWORDS: green monopropellant, droplet regression, shadow imaging, energetic ionic liquids

ABSTRACT:

Satellite attitude and orbit control manoeuvers are mostly realized by chemical thrusters, using catalytic decomposition of hydrazine. However, hydrazine is known for its carcinogenic and toxic effects and its use is thus threatened by the European chemical regulation REACh. A new monopropellant is therefore under development by CNES (the French Space Agency), and 3 proto-types are still in competition. The final choice of the best formulation will be based on real thruster tests. These new propellants are based on energetic ionic liquids, and the expected flame temperature is about 3000 K. To develop an optimized thruster demonstrator, numerical simulations, combining heat transfer and radiation in complex materials and diphasic behavior are necessary. Energetic ionic liquids have a very complex way of decomposing which explains why it is impossible to use current phase change models implemented in ONERA's multiphysics code CEDRE. A new macroscopic combustion model is being developed and implemented in CEDRE following the phenomenology of solid homogeneous propellants. Simultaneously an experiment is prepared to observe the combustion of an isolated droplet, in order to measure its regression. This experiment is a proof of concept for the final experimental CNES's setup GIMLI. This experiment will be validated on ethanol combustion and tested with the new family of green monopropellant.

GLOSSARY:

V	stationary regression rate (m.s^{-1})
a	burn rate coefficient (m.s^{-1})
n	pressure exponent (-)
P	pressure (Pa)
m_d	droplet mass (kg)
A	pre-exponential Arrhenius factor (kg.s^{-1})
E_a	activation energy (J.mol^{-1})
R	universal gas constant (J.mol^{-1}.K^{-1})
T_{surf}	surface temperature (K)
r_p	droplet radius (m)
ρ_p	particle density (kg.m^{-3})
B_T	thermal Spalding number (-)
c_p	heat capacity (J.kg^{-1}.K^{-1})
T_{gas}	gas temperature (K)
T_{dec}	decomposition temperature of mono-propellant (K)
δ	thermal penetration thickness (m)
T_δ	temperature at the thermal penetration thickness (K)
T_{moy}	mean temperature (K)
T_{sat}	saturation temperature (K)
$\Delta H_{T_\delta \to T_{dec}}$	phase change energy (J.kg^{-1})
$\phi_{conduction}$	conduction heat flux (W)
$\phi_{phase\text{-}change}$	phase-change heat flux (W)
Nu	Nusselt number (-)
λ_g	gas thermal conductivity (W.m^{-1}.K^{-1})

K_{evap} phase-change constant ($m^2.s^{-1}$)

λ_p liquid thermal conductivity ($W.m^{-1}.K^{-1}$)

1. INTRODUCTION

The European regulation on chemicals (REACh) threatens the use of hydrazine because of its highly carcinogenic and toxic effects [1]. Even though space propulsion represents a small part of the hydrazine industry, green propulsion is a major spatial research subject. Hydrazine is used since 1960 as a monopropellant without major technical innovations. Its decomposition on a Shell405 catalytic bed achieves a specific impulse of 220 s with a very high reliability. The main concern with hydrazine thrusters, except toxicity, is the catalytic bed degradation caused by thermal cycling. Because hydrazine has good performances, the requirements are very demanding for new thrusters. Electric propulsion is one of the rivals of chemical propulsion for attitude and orbit control because of its high specific impulse (2000 s) but the very low thrust of all electric technologies (Hall, ion grid, electrospray, etc.) is a major issue for high force or torque demanding manoeuvers.

Some chemical thrusters are developed to challenge the hydrazine thruster, for instance the NASA's GPIM AF-M315E [2] using Hydroxylammonium nitrate or the FOI's FLP-106 thruster based on ammonium dinitramide. Both of these thrusters use catalytic propellants based on energetic ionic liquids and increase performances from 30 to 50 % compared to hydrazine. This performance increase becomes a problem for the catalytic bed that is all the more attacked. To overcome these problems, CNES has developed an energetic ionic liquid based propellant that aims at getting rid of any catalyst. One step in the development of the new thruster is the numerical simulation of propellant combustion in the chamber to predict the heat flux on walls and finally, to design the thruster.

Ionic liquids are known to be good solvents because they do not evaporate; their saturation pressure is around 10^{-12} Pa so it is impossible to model the phase change with an Antoine's law. Furthermore, usual liquids are defined between the triple point temperature and the boiling temperature whereas ionic liquids are defined between the triple point temperature and the decomposition temperature. Therefore, usual models based on evaporation are not valid anymore and it is necessary to develop a numerical model for ionic liquid droplet decomposition. Once this model is proposed and implemented in the ONERA's code CEDRE [3], it is necessary to build an experiment to observe a droplet during its decomposition process and compare to the model.

2. DECOMPOSITION MODEL

The impetus for energetic salts decomposition began with the study of ADN (ammonium dinitramide) as a solid propellant. As presented by Thakre [4], the thermal decomposition of energetic salts is very complex to understand and simulate because the decomposition, sublimation and the gas-phase reaction are superimposed. It is thus difficult to isolate measure and understand the physics. In addition, the complex phase change releases intermediate products that will react in the gas phase with a very high reaction rate. Finally, the decomposition of energetic ionic liquids could be seen as a premixed liquid flame, without any saturation law.

2.1. Model hypothesis

The final objective is to model the heat and mass source terms of a droplet to model a complete thruster. Considering the very high reaction rate in the gas-phase caused by the premixed aspect of this energetic material, one can assume that the reaction is infinitely fast. The heat and mass source terms are fully defined by the droplet radius regression. To represent this regression, an analogy is made with solid propellants; indeed both materials are premixed energetic materials in a condensed phase. Solid propellant regression is mainly modeled with Vielle's law in stationary cases (Eq. 1) [5].

$$V = aP^n \qquad \text{Eq. 1}$$

This model is well-suited for ignition phases that are short compared to the total firing duration. In some particular cases, when the running time is short, the ignition period can't be neglected. In the case of droplets injection, the residence time is very short and it may be interesting to model ignition. Once again, in analogy with solid propellants, we will consider the chemical reaction to be in an infinitely thin layer near the droplet surface. Simply put, we model the condensed phase, receiving the heat of the exothermic decomposition

of the liquid itself, and of the burned gas. The limiting process in this decomposition is the heat transfer in the liquid phase, so we will consider that all the other phenomena are instantaneously adapted. In the end, the model is a heat transfer model in the condensed phase and the ignition is modeled by an Arrhenius law (Eq. 2):

$$\frac{dm_d}{dt} = A\, exp\left(\frac{-E_a}{RT_{surf}}\right) \qquad \text{Eq. 2}$$

2.2 Model implementation

The CEDRE code is developed by ONERA for research calculations and industrial applications. The chosen strategy to model the radius regression is the evaporation and combustion of isolated droplets, based on the D^2 law. In a D^2 approach, we can rewrite the stationary and ignition equations as below:

$$\frac{d\, {r_p}^2}{dt} = 2 r_p a P^n \qquad \text{Eq. 3}$$

$$\frac{d{r_p}^2}{dt} = \frac{1}{2 r_p \rho_p \pi} A\, exp\left(\frac{-E_a}{RT_{surf}}\right) \qquad \text{Eq. 4}$$

A transition term β, depending on the surface temperature, is then introduced in order to switch from the ignition model (Eq. 4) to the stationary model (Eq. 3).

$$\beta = f(T_s)\,, \begin{cases} \beta = 0 \;\; ignition\; model\; only \\ \beta = 1 \;\; stationary\; model\; only \end{cases}$$

$$\frac{d{r_p}^2}{dt} = A \frac{(1-\beta)}{2 r_p \rho_p \pi} exp\left(\frac{-E_a}{RT_{surf}}\right) + 2\beta r_p a P^n \qquad \text{Eq. 5}$$

The f function will be defined experimentally. The D^2 equation is finally implemented as a single equation (Eq. 5). The heating model is very important in this heat transfer problem as well. To model the heating of droplets, CEDRE uses the thermal Spalding number which is defined as the ratio between the heating flux absorbed and the phase change energy. The absorbed heat flux is defined as (Eq. 6):

$$c_p(T_{gas} - T_{dec}) \qquad \text{Eq. 6}$$

The decomposition temperature is measured by differential scanning calorimetry. The phase change energy is the heat necessary to decompose the surface layer of the droplet. As for solid propellants, one can define a thermal penetration thickness δ which depends on the thermal diffusivity and the burning rate (Fig. 1Figure 1: Thermal penetration thickness). In the case of a high regression rate, which is expected for our energetic ionic liquid, the thermal penetration thickness is very small. Therefore, we define the phase-change energy as the energy necessary to heat the δ thickness from the penetration thickness temperature to the decomposition temperature (Eq. 7).

$$\Delta H_{T_\delta \to T_{dec}} = c_p(T_\delta) \cdot (T_{dec} - T_\delta)_\delta \qquad \text{Eq. 7}$$

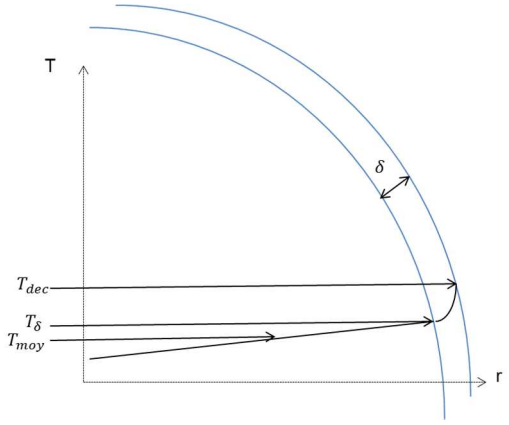

Figure 1: Thermal penetration thickness

The heating model of the condensed phase stays unchanged; we consider a conduction heating model in the droplet, to calculate the mean temperature of the droplet and its surface temperature. The first principle of thermodynamics describes the heat exchange between the gas and the droplet (Eq. 8).

$$m_d c_p \frac{dT_{moy}}{dt} = \phi_{conduction} + \phi_{phase\text{-}change} \qquad \text{Eq. 8}$$

We define a heating constant τ_c and a saturation temperature to rewrite the equation Eq. 8 into equation Eq. 9.

$$\frac{dT_{moy}}{dt} = \frac{T_{sat} - T_{moy}}{\tau_c} \qquad \text{Eq. 9}$$

With

$$\tau_c = \frac{2r_p c_p \rho_p}{3Nu\lambda_g}$$

$$T_{sat} = T_{gas} - \rho_p . K_{evap_p} . \frac{\Delta H_{T_\delta \to T_{dec}}}{Nu . \lambda_p \left[\frac{ln(1+B_T)}{B_T}\right]}$$

It is now necessary to determine the 5 coefficients: T_{dec}, A, E_a, a, n and the f function experimentally to feed the model.

2.3 Coefficients determination

The most important parameter to measure for these energetic ionic liquids is the decomposition temperature because it is the strict condition for the liquid to exist. This decomposition temperature can be measured by Differential Scanning Calorimetry and is about 450 K for our liquids. Then we have to find Arrhenius coefficients for the ignition model. The titration method can not be used in our case because the energetic salt can be considered as a premixed liquid, and a dilution could misrepresent the decomposition reaction. The kinetic parameters will be obtained by the isoconvertional analysis method, which is usually employed for pyrolysis measurement. The isoconvertional analysis can be based on different basic experimental setups such as differential thermal analysis (DTA), or thermogravimetry (TG) [6]. This analysis aims at determining the Arrhenius parameters with a model-free methodology, comparing identical conversion states with various heating speeds.

3. EXPERIMENTAL SETUP

At this step, the observation of the decomposing ionic liquid becomes necessary. First of all, because we want to observe the decomposition phenomena, ionic liquids have different paths of decomposition that impacts their phase change. The numerical model assumes the existence of an ignition step and a stationary regression, in analogy with solid propellants; an observation of the regressing liquid would permit to check if these two stages of decomposition appear. Finally, the parameters of the stationary phase, if it exists, are not defined. These parameters are necessary if we want to model a stationary regression of a liquid droplet. These parameters may depend on the pressure. For these three reasons, we started building an experiment to observe a regressing droplet, hanging on platinum fibers.

3.1. Droplet regression measurement

Observing the combustion or the decomposition of a droplet is a challenge in many applications. Unlike solid propellants, it is not possible to place a sample on a surface, inhibit it on all surfaces but one, and observe it. A possible solution to observe a droplet is by hanging it on thin crossed fibers. This support can induce a new heat flux from the droplet to the fibers, changing the regression rate. A study has been carried out by Y.C. Liu *et al.* [7] on the effect of support fibers in droplet combustion [8]. They highlighted that the thicker the fibers are, the lower the thermal diffusive time scale is. After several experiments with different fiber thicknesses, and a comparison with ISS experiments, they found that below 14 µm, the effect of the support fiber can be neglected for n-decane droplet combustion.

In our case, the ionic liquids can be considered as premixed liquid flames which are supposed to burn faster than diffusive flames. A new minimum fiber thickness has therefore to be determined for our products – expected to be greater than 14 µm. In a first part, 100 µm thick fibers are used for the experiment adjustment. The heat source is a solenoid coil with a diameter of 5 mm realized with a 0.5 mm thick piano string. The power supply is a Lambda GEN1500W Regulated power supply. In order to measure the regression of the droplet, it is necessary to visualize the edge of the droplet; therefore the shadow imaging technique is set up. The issue of shadow imaging is to enlighten more than all the other light source of the experiment. First experiments pointed out that the exothermic flame is not limiting but the light emitted by the solenoid is important. Finally, we opted for a 1200 W MK2 Cinepar metal-halide lamp at a 1 meter distance of the droplet, with a matted PMMA filter between them (Fig. 2).

Now that the light source is defined, an appropriate camera has to be chosen. Preliminary tests were realized with a 0.5 ms shutter speed which was too slow and was finally replaced by an Optronics CamRecord CR4000x2 which is able to reach a 2 µs shutter speed and 3000 fps with a 256*256

resolution. A 200 mm lens is used to have a 1.8*1.8 mm window.

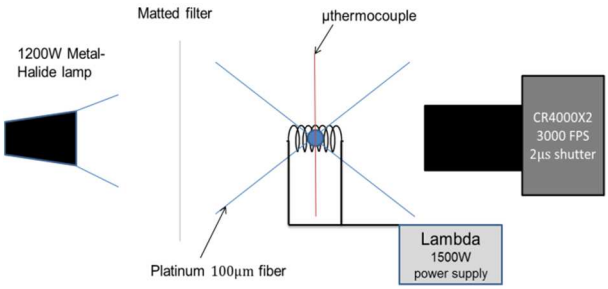

Figure 2: Schematic diagram of the experimental setup

3.2 Temperature measurement

The new decomposition model has been built as a thermal problem. Therefore, the temperature profile is crucial for the ignition model validation. Usual techniques for droplet temperature measurements such as laser-induced phosphorescence assume a constant temperature along the radius. A large difference between the average temperature of the droplet and the surface temperature is expected because the thermal penetration thickness is supposed to be small.

In a setup where the droplet is motionless, it is possible to fix a thermocouple inside. If the thermocouple is placed initially at the core of the droplet, it will sense first the core temperature of the droplet. At the end of the regression, the penetration thickness δ will reach the thermocouple that will be able to measure the final surface temperature. The first issue encountered with the use of a thermocouple is its size inside the droplet. As a matter of fact, we introduce a metallic body inside the droplet, which can induce a thermal loss and modify the droplet shape. To avoid this problem, the thermocouple has to be as small as possible. The preliminary results are realized with a 400 µm type K thermocouple probe (Fig. 3) but this will be replaced by a 12.7 µm probe at a later stage.

The second issue with thermocouples is the cut-off frequency which is inversely proportional to the volume of the probe. Even if the response time is large in liquids, the probe has to be, again, as thin as possible for the best time resolution. Microthermocouples types K with a 12.7 µm thickness have been manufactured and their cut-off frequency reaches about 100 Hz in a stationary gas [9].

Figure 3: 400 µm thermocouple in suspended droplet

3.3 Preliminary results

3.3.1 Contrast and accuracy

Preliminary results have been obtained with water, to test the setup. The first image (Fig. 4.a) illustrates the problem of a low intensity light compared to the solenoid one. With the first configuration, the contrast was not sufficient enough to enable image processing. The second image (Fig. 4.b) displays a better contrast level with the new setup. Some tests have been realized with n-decane and ethanol combustion and a good contrast is still observed even with the flame.

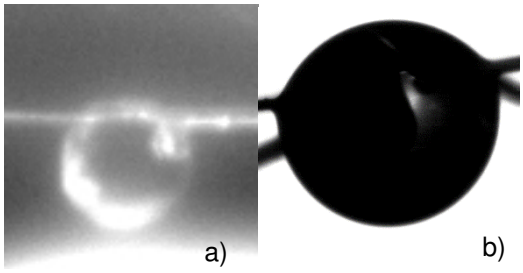

Figure 4: Improvement of shadow imaging with a new experimental setup

To reach the best possible accuracy, a 46 mm extension ring has been added to the 200 mm camera lens and the window has been set to 300*300. These final settings enable us to reach a 6.7 µm per pixel accuracy and thus the initial droplet radius is captured with 240 pixels.

3.3.2 Droplet regression

Preliminary tests have been done with water, ethanol and n-decane. Here we present the experimental results for water evaporation along with the results from computations.

The final objective is to simulate the combustion of a green propellant inside a combustion chamber. This first experiment will be used to validate the

experimental setup, by a comparison with the CGIT code developed at ONERA. CGIT is a zero-dimensional code for evaporation and combustion based on the isolated droplet model [10] [11]. So far, the vaporization of an isolated water droplet has been simulated. The initial conditions are the diameter of the droplet 1.56 mm, the droplet temperature 13 °C and the pressure 1 bar. As we do not know the heat flux received by the droplet at each instant in this one-way coupling model, the gas phase temperature profile has been set thanks to the input data from measurements. Natural convection, conduction through the thermocouple and the fibers, infinitely fast conduction inside the droplet and radiation coming from the heated coil are considered during the computations.

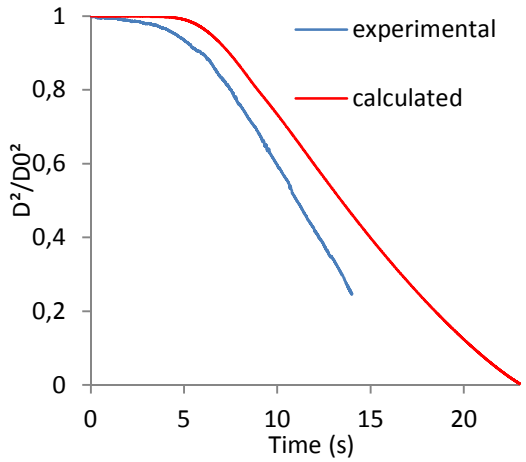

Figure 5: Comparison of D² evolution between calculation and experiment

We present here the experimental results for radius regression. The results of the calculations are compared to the temperature measurements in Fig.6. The experimental radius curve doesn't reach zero because of the thermocouple size. However, the regression rate is underestimated by the numerical simulation. The presence of the thermocouple could be the main reason for this difference, firstly because the radius doesn't regress to zero, and then because the conduction effects explained in part 3.2.3 change the droplet temperature and therefore the regression rate. These problems could be improved with thinner fibers and probe.

3.3.3 Temperature results

The temperature measured by the thermocouple is assumed to be close to the mean droplet temperature as the temperature does not vary much inside the droplet and the thermocouple is large. The temperature starts at 303 K because the acquisition by the thermocouple is triggered at this temperature and the end of the curve indicates the end of the regression measurements – in other words, when the thermocouple is not able to measure the droplet temperature. The droplet is not physically isolated from the ambient air; therefore it is subject to aerothermal effects that can deform it. If the thermocouple happens to be not perfectly inside the droplet, fluctuations around the equilibrium are observed. Apart from these fluctuations, the calculated temperature profile matches quite fairly the experimental data (Fig. 6).

However, the rate of vaporization is too low. Indeed, Fig. 5 shows that the droplet regression time is overestimated by the calculations. Several reasons can explain this error. First, the radiation from the solenoid to the droplet is probably underestimated as we do not know the temperature of the solenoid yet. Second, the thermocouple inside the droplet is so large that it can heat up the droplet by conduction more than expected and even by absorbing more radiations than water would do.

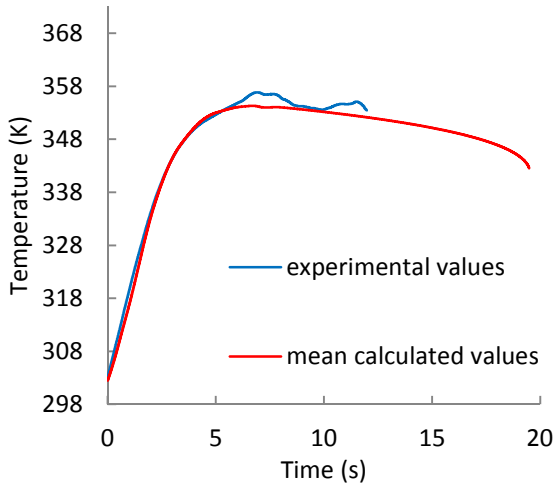

Figure 6: Comparison of mean temperature calculated with experimental thermocouple temperature

The simulations could be improved if the heat flux received by the droplet from the solenoid is known. Therefore, future computations will be needed to estimate it and implement it as input data in the current CGIT code. Increasing the power of the

radiative heat source should not modify the temperature profile significantly as the radiation becomes important only after the solenoid has reached a really high temperature and the equilibrium surface temperature is governed essentially by the diffusion of water vapor into the air. With the improvements of the measurement setup, the main causes of errors may be eliminated. In addition, the use of this code to compare with the measurements of the combustion of ethanol and kerosene would validate the current method even more. Once validated for these well-documented fuels, the combustion modeling of the green propellant would start. Simultaneously, CEDRE is used to perform the same simulations. Because it is a 3D CFD code, it will be used, eventually, to carry out simulations in more complex geometries with the injection of a fine spray of this green propellant.

4. CNES5 FIRST IMAGES

CNES5 is the first candidate tested among the 3 prototypes. A first ignition of CNES5 has been carried out in the last setup. The objective of this experiment was to observe the ignition process when heated by a solenoid. The first step of the regression is the formation of little droplets, ejected from the suspended droplet. After a certain time, the ejected droplet grows and finishes by exploding either in other droplets (Fig.7 img. 1-2 & 7-14), or directly in gas (Fig.7 img. 4 to 6). Finally the droplet is totally distorted (Fig.7 img.15) and finishes by exploding (Fig.7 img.16).

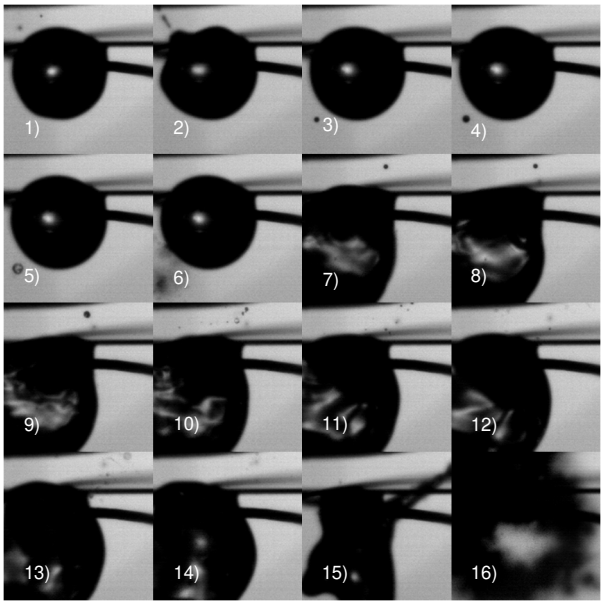

Figure 7: CNES5 droplet decomposition

These first CNES5 images can not be used to calculate a regression rate because the droplet doesn't remain spherical when the decomposition starts. This strong distortion could be induced by a decomposition starting inside the droplet and not on the surface, caused by the heating process. Indeed, the solenoid heating could be mostly radiative and the droplet surface cooled by aerothermal effects. To avoid these possible effects and to obtain a radial regression, a new experimental setup (GIMLI) is manufactured. GIMLI (Fig. 8) is a closed reactor with three optical accesses and two other flanges for the solenoid power supply and the droplet injection. A buffer volume coupled to a pressurization system permit to control the pressure during the experiment. This new setup will permit to test new heating systems.

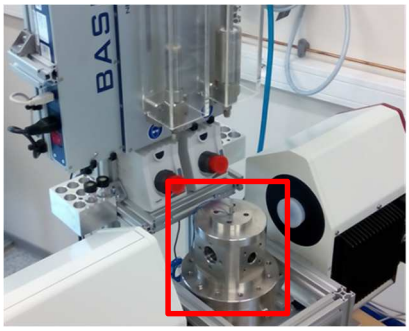

Figure 8: GIMLI experimental setup and its reactor (red square)

5. CONCLUSION

With the final aim of designing a new monopropellant thruster demonstrator, a numerical model has been built on an analogy with solid homogeneous propellants. This model had been divided into an ignition model and a stationary model. Then, to validate this model it is necessary to observe a decomposing droplet. We designed a first experimental setup to observe the possible two regimes of decomposition and validate the model coefficients. This setup had been tested with water, ethanol and n-decane and we presented in this paper a first validation for water evaporation. Even if first experiments of water evaporation are in good agreements with numerical simulations, it is necessary to improve the experimental setup by reducing the size of the suspension fibers and the thermocouple to reduce the flux passing through fibers. The CNES GIMLI setup is designed to support thinner fibers and control the pressure. This new setup also permits to reduce the aerothermal effects with a closed reactor. A first ignition

of the CNES5 monopropellant highlights a decomposition path very different from usual fuels and shows that an adaptation of the heating setup to reach a radial decomposition is necessary. However, the decomposition temperature measured with the thermocouple inside CNES5 is in good agreement with theoretical temperature.

ACKNOWLEDGMENT

This research was conducted in the context of the CNES collaboration on green monopropellant research. The authors would like to thank Christophe Corato, Juliette Aubrée for the fruitful discussions during the test.

6. REFERENCES

[1] S. Tissot et A. Pichard, «Seuils de toxicité aiguë hydrazine (NH2NH2) - INERIS-DRC-02-25590-ETSC- STi -,» Ministère de l'écologie et du développement durable ministère de la santé, de la famille et des personnes handicapées, 2003.

[2] R. A. Spores, R. Masse et S. Kimbrell, «GPIM AF-M315E Propulsion system» *49th AIAA/ASME/SAE/ASEE Joint Propulsion Conference & Exhibit,* 2013.

[3] A. Refloch, B. Courbet , A. Murrone, P. Villedieu, C. Laurent, P. Gilbank, J. Troyes, L. Tessé, G. Chaineray, J. Dargaud, E. Quémerais et F. Vuillot , «CEDRE Software» *ONERA Aerospacelab Journal,* 2011.

[4] P. Thakre, Y. Duan et V. Yang, «Modeling of ammonium dinitramide (ADN) monopropellant combustion with coupled condensed and gas phase kinetics,» *Combustion and flame,* vol. 161, issue 1, pp. 347-362, 2014.

[5] P. Vieille, «Etude sur le mode de combustion des substances explosives,» 1893.

[6] S. Vyazovkin et C. A. Wight, «Isothermal and non-isothermal kinetics of thermally stimulated reactions of solids» *International reviews in physical chemistry,* vol. 17, issue 13, pp. 407-433, 1998.

[7] Y. Liu, Y. Xu, C. Avedisian et M. Hicks, «The effect of support fibers on micro-convection in droplet combustion experiments» *Proceedings of the combustion institute,* vol. 35, issue 2, pp. 1709-1716, 2015.

[8] C. Chauveau, F. Halter, A. Lalonde et I. Gökalp, «An experimental study on the droplet vaporization: effects of the heat conduction through the support fiber,» chez *ILASS*, Como Lake, 2008.

[9] G. Lalizel et G. Arlaud, *Caractérisation spectrale de µthermocouples K de 7.6 µm pour une application aux mesures de fluctuations de température dans des écoulements anisothermes turbulents.,* Chasseneuil: LET (ENSMA).

[10] N. Doué , Modélisation de l'évaporation d'une goutte multi-composants, Toulouse, 2005.

[11] O. Rouzaud, «Concentration de vapeur et mélange; ONERA technical report: RT 1/24093,» 2017.